Aerosol indirect effect over Indo-Gangetic plain

S.N. Tripathi*, A. Pattnaik, Sagnik Dey

Department of Civil Engineering, Indian Institute of Technology, Kanpur 208016, India

Abstract

Moderate resolution imaging spectroradiometer (MODIS) data are analyzed over the Indo-Gangetic plain (IGP) to study the effect of aerosol optical depth (AOD) on the water ($R_{eff,w}$) and ice ($R_{eff,i}$) cloud effective radius for the period 2001–2005. The temporal variation of $R_{eff,w}$ and $R_{eff,i}$ shows reverse trend as that of AOD for most of the time. The intensity of positive indirect effect (i.e. increase of $R_{eff,w/i}$ with decrease of AOD and vice versa) is the highest in winter ($\Delta R_{eff,w}/\Delta AOD \sim -9.67\,\mu m$ and $\Delta R_{eff,i}/\Delta AOD \sim -12.15\,\mu m$), when the role of meteorology is the least. The positive indirect effect is significant in 43%, 37%, 68% and 54% of area for water clouds in winter, pre-monsoon, monsoon and post-monsoon seasons, respectively, whereas the corresponding values for ice clouds are 42%, 35%, 53% and 53% for the four seasons, respectively. On the contrast, $R_{eff,i}$ in some locations shows increment with the increase in AOD (negative indirect effect). The negative indirect effect is significant at 95% confidence level in 7%, 18%, 9% and 6% grids for winter, pre-monsoon, monsoon and post-monsoon seasons, respectively. The restricted spatial distribution of negative indirect effect in IGP shows that the cloud microphysical processes are very complex. Our analyses clearly identify the contrasting indirect effect, which requires further *in situ* investigations for better understanding of the aerosol–cloud interaction in the region.

© 2007 Elsevier Ltd. All rights reserved.

Keywords: Indo-Gangetic plain; Aerosol indirect effect; Clouds

1. Introduction

Aerosols indirectly affect the climate by acting as cloud condensation nuclei (CCN) and ice nuclei (IN) and thereby modify the cloud properties (Lohmann and Feichter, 2005; Koren et al., 2005). The Intergovernmental Panel on Climate Change report (Ramaswamy et al., 2001) has emphasized the importance of quantifying the indirect effect on water and ice clouds in regional scale to minimize the uncertainty in the global estimate of indirect forcing. The Twomey effect (or the 'first' indirect effect, Twomey, 1959) refers to enhanced reflection by smaller cloud droplets with fixed liquid water content, thus increasing cloud albedo. Subsequently, the more but smaller cloud droplets reduce the precipitation efficiency and increase the cloud lifetime ('second' indirect effect). Another effect (semi-direct effect) results from the absorption of solar radiation by aerosols, which heats up the atmosphere and evaporates the cloud droplets. The indirect aerosol effect has been investigated through observational as well as modeling studies in many parts of the world (Lohmann and Feichter, 2005

*Corresponding author. Tel.: +91 512 259 7845;
fax: +91 512 259 7395.
E-mail address: snt@iitk.ac.in (S.N. Tripathi).

and references therein; Myhre et al., 2006). In Indian subcontinent, during the Indian Ocean Experiment, this issue was addressed for the Indian Ocean (Ramanathan et al., 2001), where the polluted clouds have aerosol number density three times larger than that in the pristine clouds. Subsequently, Vinoj and Satheesh (2004) have studied the indirect effect of sea salt aerosols on the cloud microphysical properties over the Arabian Sea using the empirical relations developed from the INDOEX measurements. But no previous study was focused to the Indo-Gangetic plain (IGP), where the aerosol characteristics are complex due to mixing of anthropogenic and natural aerosols (Chinnam et al., 2006).

Here, we focus on IGP, which is the most polluted region in the Indian sub-continent (Singh et al., 2004; Tripathi et al., 2005a, b) and contribute to the wintertime pollution observed over the adjacent oceans. The most striking feature of the IGP is that mineral dust adds to the anthropogenic pollution load in the pre-monsoon and monsoon seasons (Dey et al., 2004; Chinnam et al., 2006). The effect of the increasing pollution load on the water and ice clouds could be different, as observed recently by Chylek et al. (2006) using moderate resolution imaging spectroradiometer (MODIS) data over the Indian Ocean during the winter months. In this paper, spatial and temporal inter-relationship between aerosol optical depth (AOD, quantifying the pollution load) and effective radius of water ($R_{eff,w}$) and ice clouds ($R_{eff,i}$) has been explored to study the aerosol indirect effect in the IGP. However, aerosol–cloud interaction is not straightforward; as aerosols and clouds are related also other than through microphysics, most notably through their dependence on meteorological conditions. The meteorological effect has been decoupled from the aerosol effect using the NCEP vertical wind data (Koren et al., 2005). The main objectives of this paper are to investigate the intensity and spatial extent of the indirect effect in the IGP and to identify if the indirect effects for water and ice clouds show any contrasting behavior.

2. Study area and data analysis

In our analysis, to account the spatial variation, the IGP has been divided into four regions (Fig. 1a). First region (70–76°E and 22–32°N) represents the western part of IGP which includes the Thar desert region, which is the major dust producing area
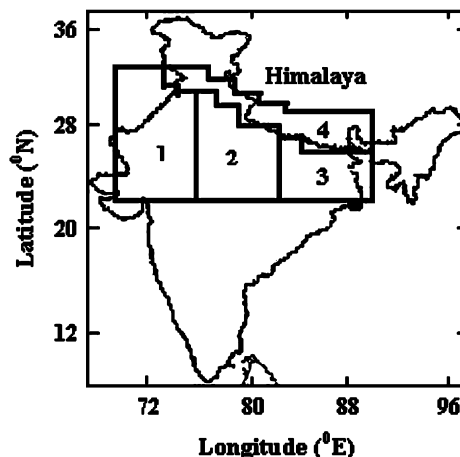

Fig. 1. The area covered under the four regions in the IGP chosen in the present study.

(Chinnam et al., 2006). Second region (76–82°E and 22–30°N) covers the central part of the IGP and third region (82–91°E and 22–28°N) comprises the eastern part of IGP. A fourth region is separated from the main IGP and defined as the foothills of the Himalayas. Each region is further sub-divided into grids of $1° \times 1°$ and analysis has been performed for each grid. The current analysis in larger spatial grids is able to capture the general trend and indicates some interesting discrepancies, which indicates the necessity to perform similar analysis in much finer spatial scale along with *in situ* data to have more accurate quantification of the indirect effect in this region. Also, it should be kept in mind that clouds observed in a particular grid might have been transported from another location, which is not possible to account for using the satellite data and is a limitation of this study. However, we have considered five year time period and statistically significant correlation between AOD and cloud effective radius would indicate that this could not be an artifact. The grids covering the Himalayan mountainous region in the north of IGP and the fourth region are excluded from the statistical analyses, as they do not represent the basin and the topographic nature of the terrain along with the orographic influence would make the aerosol–cloud interaction study using the satellite data problematic.

The aerosol and cloud parameters are extracted from the level-3 MODIS-Terra gridded atmosphere monthly global product (Kaufman et al., 1997; Platnick et al., 2003) for each grid for a period of 5

years (2001–2005). Level 3 monthly data are produced by averaging the daily aerosol and cloud products at $1° × 1°$ grid and available in MODIS online visualization and analysis system (http://g0dup05u.ecs.nasa.gov/Giovanni/). Comparison with ground based AERONET measurements, MODIS AOD (at $0.55 \mu m$) product was found to be within the retrieval errors of $\Delta \tau_a = \pm 0.2\tau_a \pm 0.05$ (Chu et al., 2002). However, Tripathi et al. (2005c) have shown that MODIS overestimates AOD during the summer months over the IGP. They have found that the absolute error in MODIS AOD is ~25% of the absolute value of MODIS AOD as compared to the AERONET AOD. Very high aerosol loading (AOD > 0.6) could lead to aerosol contamination in the cloud retrieval (Brennan et al., 2005). In winter and post-monsoon seasons, AOD remains less than 0.6 in the IGB, means that the aerosol contamination would not affect the data to study the AOD and R_{eff} correlation. However, during the pre-monsoon season in the first region and during the monsoon season, this effect would cause an underestimation of the rate of the indirect effect (shown in Table 1 and discussed afterwards). The overall signature of the indirect effect although would not be altered.

First, several cloud detection tests are performed to judge whether any particular pixel is cloudy or not (Platnick et al., 2003) and once it is confirmed as cloudy pixel, the cloud parameters are retrieved. The cloud optical depth, COD and R_{eff} are retrieved simultaneously by matching the satellite-measured spectral reflectance with the theoretical estimations of reflection function (function of COD and R_{eff}) using a radiative transfer algorithm (Platnick et al., 2003). The parameters are retrieved using the water-absorption bands of 1.6, 2.1 and $3.7 \mu m$ along with one of the non-absorbing (0.65, 0.86 and $1.2 \mu m$)

Table 1
Rate of change of $R_{eff,w/i}$ with AOD, when the positive indirect effect was considered statistically significant at 95% confidence level and their spatial extent

Seasons	$(\Delta R_{eff,w/i})/\Delta AOD$	Spatial extent (%)
Winter	−9.67, −12.15	43, 42
Pre-monsoon	−5.3, −8.63	37, 35
Monsoon	−7.47, −7.5	68, 53
Post-monsoon	−9.5, −10.22	60, 53

In both the columns, first value is for water clouds and the second one is for ice clouds. The negative sign indicates their inverse relationship. Spatial extent of significant is expressed in terms of percentage of area with respect to the total IGP.

bands at 1 km resolution (level 2 data). R_{eff} is retrieved separately for water ($R_{eff,w}$) and ice ($R_{eff,i}$) clouds after determining its phase using bi-spectral infrared algorithm (Platnick et al., 2003). The brightness temperature difference between 8.5 and $11 \mu m$ bands is positive for ice phase and negative for water phase, as shown by radiative transfer calculations. If the satellite detects multilayered clouds, the cloud phase classification algorithm returns 'mixed-phase' status.

Like every data set, MODIS also has uncertainty in absolute values of the retrieved geophysical parameters (e.g. satellite-retrieved R_{eff} is generally higher than the *in situ* measured value). The uncertainty in the retrieval of COD and R_{eff} originates from either the modeled reflection function lookup tables or the physical uncertainties resulting during the atmospheric corrections at different wavelengths. The model uncertainty of R_{eff} is ~$0.5 \mu m$ for $R_{eff} < 20 \mu m$. Wavelength integration over band pass filters is a potentially significant source of errors in retrieval of COD and R_{eff}. Uncertainty analysis reveals that for COD~50, error in R_{eff} is less than $0.1 \mu m$, but for optically thin clouds (COD~1), error in R_{eff} is higher (~$0.3 \mu m$). Overall, the retrieval uncertainty is large for smaller values of COD and R_{eff}. The physical uncertainty in R_{eff} is in between 1 and $3 \mu m$ for optically thick clouds. Radiative transfer computations by Nakajima and King (1990) at 0.75, 1.65 and $2.16 \mu m$ have shown that the overall error in the reflection is ~5%. The general tendency is that if there is error in COD, there would be error in R_{eff}, e.g. the error in COD can reach up to $\pm 25\%$ for an error of $\pm 50\%$ in R_{eff}. In general, the error is less for single layer cloud retrieval and increases for mixed-phase multilayered clouds (King et al., 1998). The retrieval error of cloud top pressure (CTP) is 50 hPa for clouds present at more than 3 km height, error being higher for lower clouds (~150 hPa) (Platnick et al., 2003). Keeping in mind the uncertainty and the limitations of the MODIS aerosol and cloud products, we have carried out grid-based analysis to investigate the aerosol indirect effect.

The clouds were classified as low (CTP > 680 hPa), medium (440 hPa < CTP < 680 hPa) and high (CTP < 440 hPa) following the International Satellite Cloud Climatology nomenclature (Doutriaux-Boucher and Séze, 1998). Further the three classes were subdivided into 9 based on the optical thickness, where the optically low clouds have
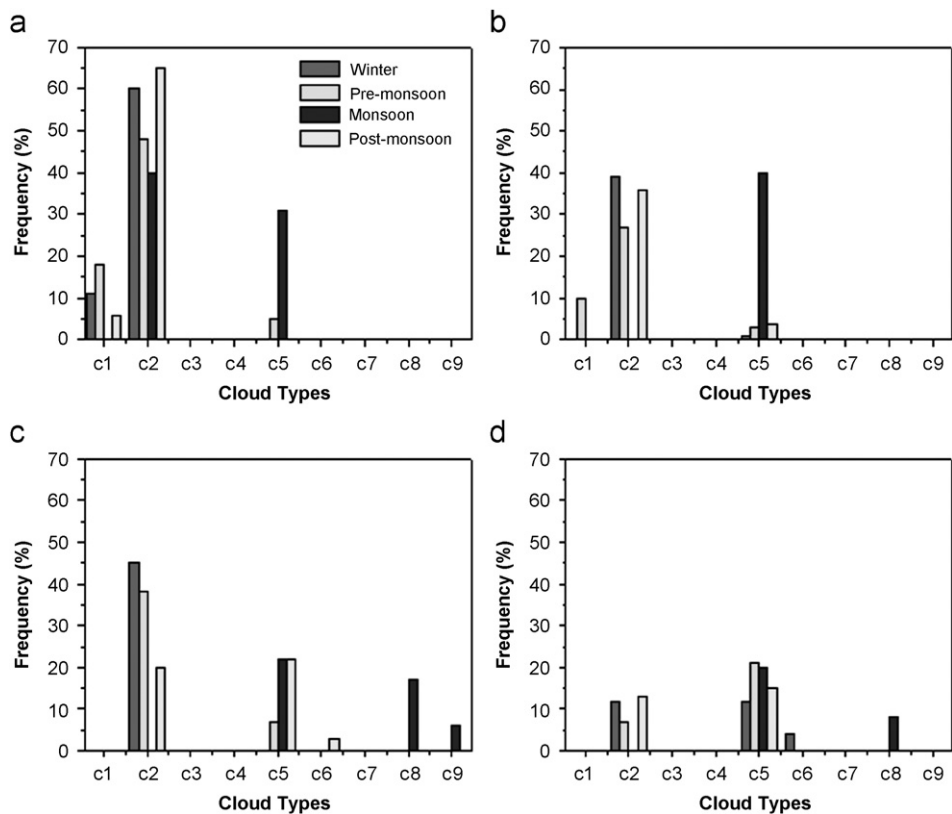
Fig. 2. Frequency distribution of cloud types for different seasons in: (a) first, (b) second, (c) third, and (d) fourth region of IGP, respectively.

$COD < 3.2$, medium clouds are in the range $3.2 < COD < 23$ and optically high clouds have $COD > 23$. The frequency distributions of cloud types in four regions are illustrated in Fig. 2. In the IGP, low level clouds dominate in the winter (December–February, 77%) and post-monsoon (September–November, 61%) seasons, whereas, high level clouds are significant in the monsoon season (June–August, 30%). Mid level clouds vary from a low 23% in the winter to a high 46% in the monsoon season. In the pre-monsoon season (March–May), low level clouds are found to exist in 58% grids followed by mid-level clouds in 40% grids. In the statistical analysis, $R_{eff,w}$ and $R_{eff,i}$ have been considered, respectively, for investigating the indirect effect of aerosols on water and ice clouds.

3. Results and discussions

To account for the aerosol indirect effect, we have studied the inter-relationship between AOD and $R_{eff,w/i}$ separately for each season, both in temporal and spatial scale. R_{eff} decreases with increase in

aerosol flux and vice versa as commonly expected, which is termed as positive (or normal) indirect effect. Sometimes, R_{eff} instead of decreasing, increases with the increase in aerosol flux and is termed as negative (or reverse) indirect effect here. Positive indirect effect has been observed for larger areas on a temporal scale, whereas negative (or reverse) indirect effect has been observed, but in restricted spatio-temporal scale. The detailed results are presented in the next two sections.

3.1. Positive aerosol indirect effect

The temporal variations of the AOD, $R_{eff,w}$ and $R_{eff,i}$ averaged over first, second and third regions are illustrated in Fig. 3. $R_{eff,w}$ and $R_{eff,i}$, similar to AOD, exhibit strong seasonal variability in all three regions. AOD time series exhibits one sharp peak prior to the onset of the monsoon season for all the regions; however, the amplitude of variation is maximum in the first region. Mean annual AOD ($\pm$ standard deviation, SD) in the three regions are 0.56 ± 0.2, 0.49 ± 0.2 and 0.5 ± 0.1, respectively.
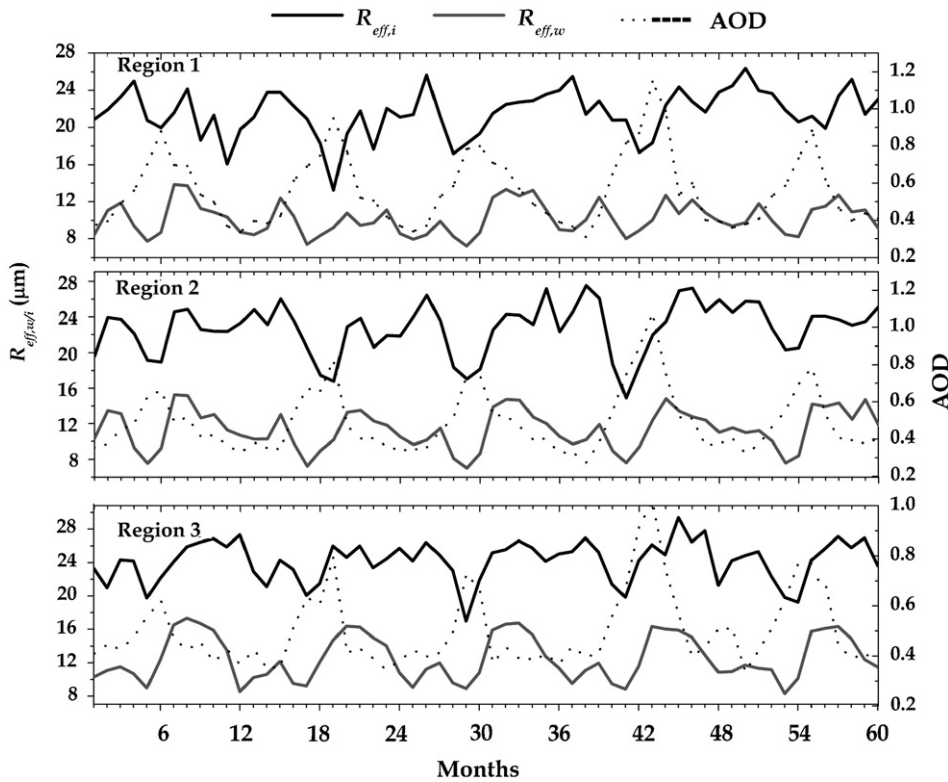
Fig. 3. Temporal variations of AOD and $R_{eff,w}$ and $R_{eff,i}$ in the three regions. Months start from January 2001 up to December 2005.

The most prominent feature of this plot is that $R_{eff,w}$ and $R_{eff,i}$ are in similar phase and both are in opposite phase to AOD for most of the months. The seasonal average ($\pm$SD) of $R_{eff,w}$ in the entire IGP are 10.22 ± 1.6, 10.34 ± 1.7, 12.95 ± 2.4 and $13.24\pm 2.2\,\mu m$ in winter, pre-monsoon, monsoon and post-monsoon seasons, respectively, and the corresponding $R_{eff,i}$ values are 24.08 ± 2.4, 22.6 ± 2.5, 22.45 ± 2.7 and $24.38\pm2.8\,\mu m$, respectively. $R_{eff,w}$ and $R_{eff,i}$ are lowest in the western IGP for all seasons, where AOD is maximum again indicating the indirect effect. As the aerosol loading persists throughout the year (even in the cleanest condition, AOD $\sim$0.2), amplitude of variations in $R_{eff,w}$ and $R_{eff,i}$ is much reduced as compared to the oceans (Chylek et al., 2006).

As the regional-averaged statistics overlooks the spatial-scale effect and any definite relationship, the aerosol indirect effect was investigated further for each $1^\circ \times 1^\circ$ grid in the IGP for all four seasons. First, we have considered the correlations between AOD and $R_{eff,w/i}$ in five domains of cloud fraction, η ($0<\eta<0.2$, $0.2<\eta<0.4$, $0.6<\eta<0.8$ and $0.8<\eta< 1$) for four seasons (Fig. 4) to study how the

increasing cloud fractions influence the aerosol indirect effect. It is evident from the figure that the correlation coefficient (absolute value is plotted) improves with the cloud fraction, which implies that at low cloud fraction the influence of aerosols on the cloud microphysical properties is negligible. Only for the water clouds in the winter season, the correlation does not show any change. Best correlation has been obtained in the pre-monsoon season, but the correlation coefficient of AOD and $R_{eff,w}$ for $\eta>0.6$ becomes lower. In monsoon season, no grid was found with $\eta<0.6$.

We further looked into grid-based analysis with different criteria and found that when in a particular grid, AOD exceeds the seasonal mean value and corresponding $R_{eff,w/i}$ recedes below the mean value or vice versa, the positive indirect effect becomes statistically significant at 95% confidence level. The spatial distribution of the correlation coefficient (r_w) between AOD and $R_{eff,w}$ is shown in Fig. 5a and correlation coefficient (r_i) between AOD and $R_{eff,i}$ is shown in Fig. 5b. For the water clouds, we found that 43%, 37%, 68% and 60% grids in the entire study area showed significant indirect effect in
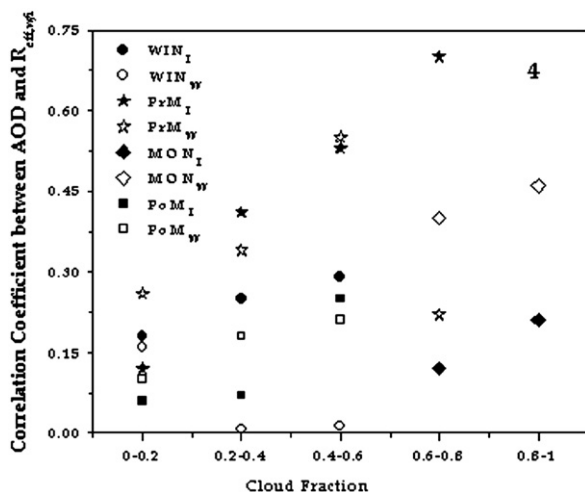
Fig. 4. Correlation between AOD and $R_{\text{eff,w/i}}$ (denoted as 'w' and 'i' in subscript) in different cloud fraction domains for winter (WIN), pre-monsoon (PrM), monsoon (MON) and post-monsoon (PoM) seasons in the IGP.

winter, pre-monsoon, monsoon and post-monsoon seasons. For the ice clouds, the corresponding percentages of the grids were 42%, 35%, 53% and 53% for the four seasons. r_{w} is high in the central part of IGP, which got elongated from west to east in the monsoon season. The insignificant r_{w} is seen to occur as patches in the winter and pre-monsoon seasons. r_{w} becomes better in the monsoon and post-monsoon seasons. On the contrary, the distribution of significant r_{i} is restricted to second and third regions mostly in the winter and pre-monsoon seasons, which shifts to first and second regions in the monsoon season and becomes restricted to the first region with patches in the third region in the post-monsoon season. The distribution of negative indirect effect is discussed in the next section. The seasonally-averaged rate of change of $R_{\text{eff,w/i}}$ with AOD and the correlation coefficients for both types of clouds are summarized in Table 1. The spatial extent of positive indirect effect is highest in the monsoon season (68% and 53% grids for water and ice clouds) and lowest in the pre-monsoon season (∼35%) for both types of clouds. On the other hand, the intensity of the positive indirect effect (as reflected by the rate of change of $R_{\text{eff,w/i}}$ with AOD) is highest for the winter season, followed by post-monsoon, monsoon and pre-monsoon seasons.

The western IGP is dominated by coarse mode aerosols, whereas the fine mode fractions (representing the anthropogenic components) dominate in the central and eastern parts, as observed from the MODIS aerosol fine mode fraction product (not shown). We also present the optical depths for individual components in the IGP as obtained from GOCART model (http://g0dup05u.ecs.nasa.gov/Giovanni/modis.GOCART.2.shtml) for the first three regions (Fig. 6) to provide an estimate of the chemical composition of aerosols. We exclude the fourth region for two reasons; first, AOD is always the lowest in this region and hence not providing enough particles to influence the cloud properties and secondly, the clouds are influenced by orographic effect. Among the four major components, dusts are generated naturally, while black carbon (BC), organic carbon (OC) and sulfate are products of anthropogenic activities in the region (Tare et al., 2006; Dey and Tripathi, 2007). As expected, dust optical depth is highest in the first region in pre-monsoon season followed by monsoon season. As one moves across the IGP from west towards east, BC, OC and sulfate optical depths increase confirming higher anthropogenic pollution. The above analysis indicates that the positive aerosol indirect effect in the IGP is the strongest during winter season, when the regional pollution is mainly due to anthropogenic activities (Dey and Tripathi, 2007). The hygroscopic species such as sulfate, are mostly in fine mode (Tare et al., 2006) and serve as good CCN in the winter season in the IGP (Tare et al., 2006). On the other hand, BC and OC (if becomes hydrophilic) and dust can act as efficient IN (Demott et al., 1999). In the pre-monsoon and monsoon seasons, the effect of dust particles makes the cloud microphysical processes more complex through the interaction with other species, which affects the intensity and extent of the indirect effect.

3.2. Negative aerosol indirect effect on limited spatio-temporal scale

The most interesting finding from the grid-based analysis is that $R_{\text{eff,i}}$ behaves differently, in restricted spatio-temporal scale, showing higher values in regions having higher AOD (Fig. 7). Such effect is not observed for the water clouds. We have seen that, when $R_{\text{eff,i}}$ exceeds the seasonal mean plus standard deviation with the corresponding AOD exceeding seasonal mean, the correlation between AOD and $R_{\text{eff,i}}$ becomes significant at 95% confidence level. With a lower threshold of $R_{\text{eff,w/i}}$ set at corresponding mean as compared to mean plus standard deviation, the correlation is not significant at all regions and all seasons. Hence for negative
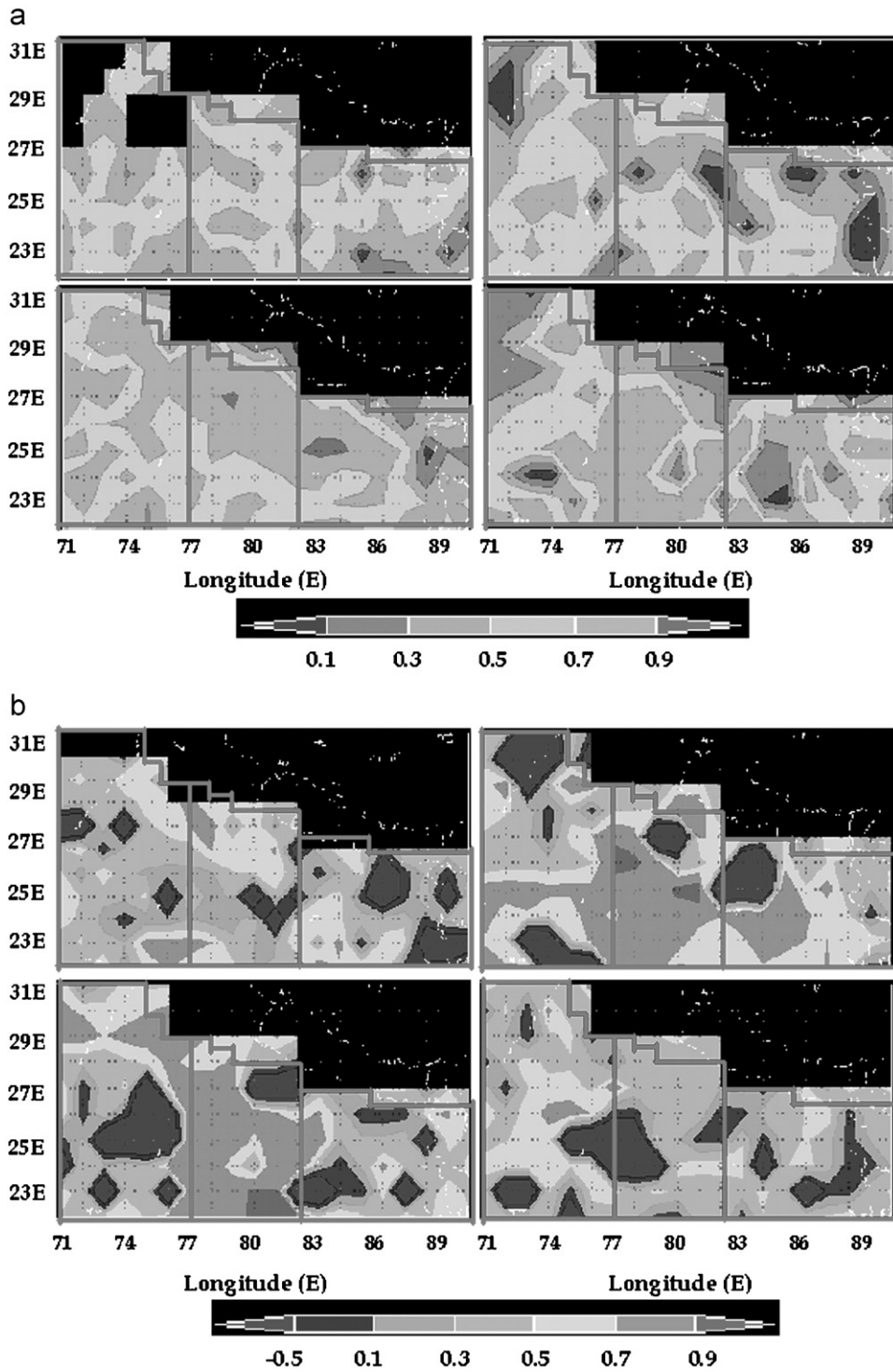
Fig. 5. (a) Spatial distribution of correlation coefficient (r_w) between AOD and R_{eff} of water clouds in winter (top left), pre-monsoon (top right), monsoon (bottom left) and post-monsoon (bottom right) seasons. $r_w > 0.5$ indicates statistically significant (at 95% confidence level) positive indirect effect. (b) Same as (a), but for ice clouds (r_i). $r_i < -0.5$ indicates statistically significant (at 95% confidence level) negative indirect effect.
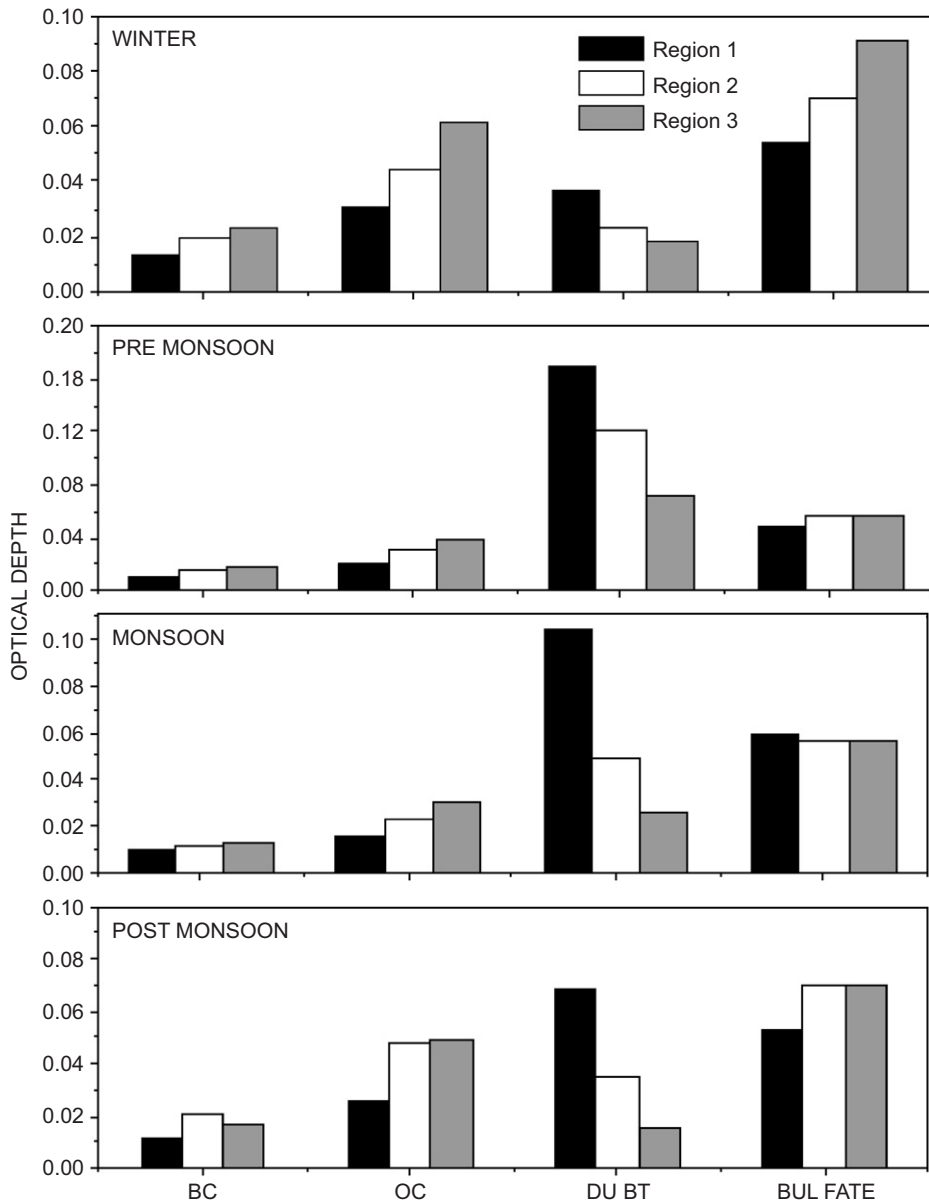
Fig. 6. Comparison of the optical depth of BC, OC, dust and sulfate in regions 1, 2 and 3 (shown as different colors) during all seasons as obtained from GOCART model.

indirect effect, the lower threshold value was discarded.

In winter season, highest $R_{eff,i}$ (27 μm) is observed in the third region (Fig. 7a), where AOD is maximum(~0.6). Similar feature ($R_{eff,i} > 25$ μm) is noted during the pre-monsoon season in a broader spatial extent, one in the same region and the other one in the northwestern IGP (top-left corner in the first region, Fig. 7b) and it is continuing in the monsoon season (follow 25 μm contour in Fig. 7c).

The effect is not so conspicuous in the post-monsoon season from Fig. 4. Spatial-scale analysis reveals that 7%, 18%, 9% and 6% grids satisfy our criteria for the negative effect in winter, pre-monsoon, monsoon and post-monsoon seasons, respectively, which is also reflected in the spatial distribution of r_i (Fig. 5b). The significant r_i for negative indirect effect is spatially restricted and appears as patches in different regions in different seasons.
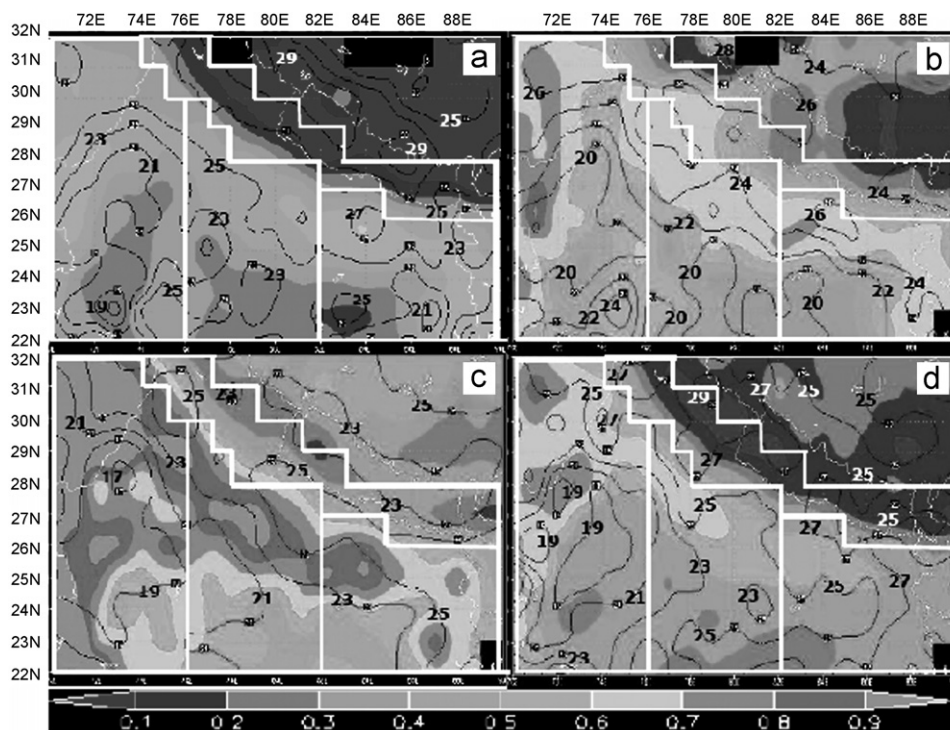
Fig. 7. Contours of $R_{eff,i}$ (values in μm written on the contour lines) in the IGP for: (a) winter, (b) pre-monsoon, (c) monsoon, and (d) post-monsoon seasons. In the background, spatial distribution of AOD is shown along with its scale.

The apparent negative indirect effect could be due to heterogeneous ice nucleation (Chylek et al., 2006). Heterogeneous ice nucleation is predicted to lead to a negative indirect effect in cirrus clouds resulting from initiation of ice nucleation at lower supersaturation than required for homogeneous freezing nucleation and a consequent formation of fewer and larger ice crystals (Jensen and Toon, 1997). The ice clouds form through either homogeneous or heterogeneous nucleation depending on the ambient meteorological conditions. Homogeneous nucleation initiates at temperature less than 235 K (Lohmann and Kärcher, 2002). Cloud-top-temperature from MODIS in this region reveals that only in July–August, it dips below 235 K, that too in only ~2% grids. This clearly suggests that these clouds formed at an altitude, where homogeneous nucleation is unlikely to occur. Since it is not possible to account for the behavior of the species in the microphysical processes, we restrict ourselves only in identifying such effect without any further quantification. But highest spatial extension of negative indirect effect is accounted in the pre-monsoon season when the mineral dust optical depth is maximum in all three regions. However, the exact mechanism through which the particles will behave as IN after mixing and play a role in the negative indirect effect is not truly known.

4. Decoupling the meteorological effect

$R_{eff,w/i}$ and AOD are not only connected through the microphysical properties, but also through the meteorology. To extricate the meteorological effect, we have analyzed vertical wind velocity, VW (as it is the most important meteorological parameter influencing cloud properties as mentioned by Koren et al. (2005)) from NCEP reanalysis data at levels closest to the mean CTP for a particular season. VW shows strong updraft in the pre-monsoon (77% grids) and monsoon (90% grids) seasons and strong subsidence in winter (67% grids), whereas in the post-monsoon season, both updrafts and downdrafts prevail almost equally. As the VW data are available in $2.5° × 2.5°$ grid, the CTP from MODIS are converted into similar resolution to study the correlation. Correlation coefficients between VW and CTP are 0.26, 0.41, 0.63 and 0.6 for winter, pre-monsoon, monsoon and post-monsoon seasons, respectively. Restricting our analysis to the grids

showing upward VW only, did not alter the correlation much.

Poor correlation ($r = 0.26$) between VW and CTP in winter suggests that the change in $R_{\mathrm{eff,w/i}}$ is less influenced by meteorology due to reduced updraft and hence it shows highest intensity of the indirect effect. This is supported by high positive correlation ($r = 0.67$, significant at 95% confidence level) between AOD and cloud fraction. In the pre-monsoon, monsoon and post-monsoon seasons, the correlations are 0.41, 0.63, and 0.6, respectively. In the monsoon, the aerosol effect is facilitated by favorable meteorological condition (strong updraft) and hence the spatial extent of positive indirect effect is the highest. Further, we have studied the inter-relationship between columnar water vapor (CWV) and cloud fraction (CF), because if convergence were responsible for accumulating aerosols in cloud formation and modification, it would also accumulate water vapor. For this purpose, we have calculated columnar water vapor from the radiosonde data as an independent measure available for Lucknow and Delhi (two locations in IGP). The poor correlation between CF and CWV for both the stations ($r = 0.03$ and 0.033, respectively, for Lucknow and Delhi) during winter suggests least influence of meteorology on aerosol–cloud interaction. The correlation improves in the other season. In the pre-monsoon season, r is significant (0.68) at 95% confidence level in Lucknow, whereas, in Delhi, it (0.36) is not. r in the monsoon season is not significant at 95% confidence level (0.41 and 0.32 for Lucknow and Delhi, respectively). However, in the post-monsoon season, the correlation is significant (0.85 and 0.67 for Lucknow and Delhi, respectively). The analysis suggests that the meteorology is not solely responsible for the cloud formation, even in the monsoon season; the aerosol effect can be identified.

Although we could not fully decouple the meteorological influence from the aerosol effect, the results identify contrasting aerosol indirect effect in the IGP, which would make the estimation of aerosol indirect forcing complex in the region. The ice clouds showing negative indirect effect have different effect on the radiative forcing (as they reflect less radiation) than the ice clouds showing positive indirect effect. Although it was not possible to estimate the separate contribution of the homogeneous and heterogeneous ice nucleation, both should be considered in the climate models for this region. Our analyses indicate the importance of further *in situ* field measurements to corroborate such complex nature of the aerosol–cloud interaction in the region.

5. Summary and conclusions

The aerosol indirect effect over the IGP are investigated through the relationship between AOD and $R_{\mathrm{eff,w/i}}$ using the MODIS data from 2001 to 2005. Keeping in mind the limitations of the data set, our analyses reveal the following facts:

1. $R_{\mathrm{eff,w}}$ and $R_{\mathrm{eff,i}}$ are in similar phase and both are in opposite phase to AOD for most of the months. Grid-based spatial-scale analyses reveal that the intensity of indirect effect for both types of clouds is highest in winter season ($\Delta R_{\mathrm{eff,w}}/\Delta \mathrm{AOD} \sim -9.67\,\mu\mathrm{m}$ and $\Delta R_{\mathrm{eff,i}}/\Delta \mathrm{AOD} \sim -12.15\,\mu\mathrm{m}$) due to least meteorological influence, whereas the spatial extent is maximum in the monsoon season.
2. $R_{\mathrm{eff,i}}$ sometimes shows increasing trend with AOD, possibly due to the aerosol effect on heterogeneous ice nucleation processes. The negative indirect effect is significant in 7%, 18%, 9% and 6% grids for winter, pre-monsoon, monsoon and post-monsoon seasons, respectively.
3. The complex nature of aerosol–cloud interaction in spatial and temporal scale in the IGP suggests the importance of further *in situ* measurements to understand the aerosol indirect effect in this region.

Acknowledgements

References

Brennan, J.I., Kaufman, Y.J., Koren, I., Li, R.R., 2005. Aerosol–cloud interaction–misclassification of MODIS clouds in heavy aerosol. IEEE Transactions on Geoscience and Remote Sensing 43, 911–915.

Chinnam, N., Dey, S., Tripathi, S.N., Sharma, M., 2006. Dust events in Kanpur, northern India: chemical evidence for source and implications to radiative forcing. Geophysical Research Letters 33, L08803.

Chu, D.A., Kauman, Y.J., Ichoku, C., Remer, L.A., Tanre, D., Holben, B.N., 2002. Validation of MODIS aerosol optical depth retrieval over land. Geophysical Research Letters, 29 (12), 1617, doi:10.1029/2001GL013205.

Chylek, P., Dubey, M.K., Lohmann, U., Ramanathan, V., Kaufman, Y.J., Lesins, G., Hudson, J., Altmann, G., Olsen, S.C., 2006. Aerosol indirect effect over the Indian Ocean. Geophysical Research Letters 33, L06806.

Demott, P.J., Chen, Y., Kreidenweis, S.N., Rogers, D.C., Sherman, D.E., 1999. Ice formation by black carbon particles. Geophysical Research Letters 26 (16), 2429–2432.

Dey, S., Tripathi, S.N., 2007. Estimation of aerosol optical properties and radiative effects in the Ganga basin, northern India during the winter time. Journal of Geophysical Research 112, D03203.

Dey, S., Tripathi, S.N., Singh, R.P., Holben, B.N., 2004. Influence of dust storms on aerosol optical properties over the Indo-Gangetic basin. Journal of Geophysical Research 109, D20211.

Doutriaux-Boucher, M., Séze, G., 1998. Significant changes between the ISCCP C and D cloud climatologies. Geophysical Research Letters 25 (22), 4193–4196.

Jensen, E.J., Toon, O.B., 1997. The potential impact of soot particles from aircraft exhaust on cirrus clouds. Geophysical Research Letters 24 (3), 249–252.

Kaufman, Y., Tanre, D., Remer, L.A., Vermote, E.F., Chu, A., Holben, B.N., 1997. Operational remote sensing of tropospheric aerosols over land from EOS moderate resolution imaging spectroradiometer. Journal of Geophysical Research 102, 17051–17067.

King, M D., Tsay, S.-C., Platnick, S.E., Wang, M. Liou, K.-N., 1998. Cloud retrieval algorithms for MODIS: optical thickness, effective particle radius, and thermodynamic phase. MODIS Algorithm Theoretical Basis Document No. ATBD-MOD-05 MOD06—Cloud product, p. 57.

Koren, I., Kaufman, Y.J., Rosenfeld, D., Remer, L.A., Rudich, Y., 2005. Aerosol invigoration and restructuring of Atlantic convective clouds. Geophysical Research Letters 32, L14828.

Lohmann, U., Feichter, J., 2005. Global indirect aerosol effects: a review. Atmospheric Chemistry and Physics 5, 715–737.

Lohmann, U., Kärcher, B., 2002. First interactive simulations of cirrus clouds formed by homogeneous freezing by ECHAM general circulation model. Journal of Geophysical Research 110 (D10).

Myhre, G., et al., 2006. Aerosol–cloud interaction inferred from MODIS satellite data and global aerosol models. Atmospheric Chemistry and Physics Discussions 6, 9351–9388.

Nakajima, T., King, M.D., 1990. Determination of the optical thickness and effective particle radius of clouds from reflected solar radiation measurements. Part I: theory. Journal of Atmospheric Science 47, 1878–1893.

Platnick, S., King, M.D., Ackerman, S.A., Menzel, W.P., Baum, B.A., Riédi, J.C., Frey, R.A., 2003. The MODIS cloud products: algorithms and examples from Terra. IEEE Transactions on Geoscience and Remote Sensing 41 (2), 459–473.

Ramanathan, V., et al., 2001. Indian Ocean Experiment: an integrated analysis of the climate forcing and effects of the great Indo-Asian haze. Journal of Geophysical Research 106 (D22), 28,371–28,398.

Ramaswamy, V., et al., 2001. Radiative forcing of climate change. In: Houghton, J.T., et al. (Eds.), Climate Change 2001: The Scientific Basis, Contribution of Working Group I to The Third Assessment Report of The Intergovernmental Panel on Climate Change. Cambridge University Press, New York, pp. 349–416.

Singh, R.P., Dey, S., Tripathi, S.N., Tare, V., Holben, B.N., 2004. Variability of aerosol parameters over Kanpur, northern India. Journal of Geophysical Research 109, D23206.

Tare, V., Tripathi, S.N., Chinnam, N., Srivastava, A.K., Dey, S., Manar, M., Kanawade, V.P., Agarwal, A., Kishore, S., Lal, R.B., Sharma, M., 2006. Measurements of atmospheric parameters during ISRO-GBP land campaign II at a typical location in Ganga basin: part II-chemical properties. Journal of Geophysical Research 111, D23210.

Tripathi, S.N., Dey, S., Tare, V., Satheesh, S.K., 2005a. Aerosol black carbon radiative forcing at an industrial city in northern India. Geophysical Research Letters 32, L08802.

Tripathi, S.N., Dey, S., Tare, V., Satheesh, S.K., Lal, S., Venkataramani, S., 2005b. Enhanced layer of black carbon in a north Indian industrial city. Geophysical Research Letters 32, L12802.

Tripathi, S.N., Dey, S., Chandel, A., Srivastava, S., Singh, R.P., Holben, B.N., 2005c. Comparison of MODIS and AERONET derived aerosol optical depth over the Ganga basin, India. Annales Geophysicae 23, 1093–1101.

Twomey, S.A., 1959. The nuclei of natural cloud formation. Part II: the supersaturation in natural clouds and the variation of cloud droplet concentrations. Geofisica Puree Applicata 43, 227–242.

Vinoj, V., Satheesh, S.K., 2004. Direct and indirect radiative effects of sea-salt aerosols over Arabian Sea. Current Science 86, 1381–1390.